

1 **Mass-dependent Selenium Isotopic Fractionation during Microbial Reduction of**
2 **Seleno-oxyanions by Phylogenetically Diverse Bacteria**
3

4 Kathrin Schilling^{1*}, Anirban Basu², Christoph Wanner³, Robert A. Sanford⁴, Celine Pallud⁵,
5 Thomas M. Johnson⁴, Paul R.D. Mason⁶
6

7 ¹ *Lamont-Doherty Earth Observatory of Columbia University, Palisades, NY, USA*

8 ² *Department of Earth Sciences, Royal Holloway, University of London, Egham, TW20 0EX,*
9 *United Kingdom*

10 ³ *Institute of Geological Sciences, University of Bern, Baltzerstrasse 3, CH-3012 Bern,*
11 *Switzerland*

12 ⁴ *Department of Geology, University of Illinois at Urbana-Champaign, Champaign, IL,*
13 *61820, USA*

14 ⁵ *Department of Environmental Science, Policy and Management, University of California,*
15 *Berkeley, 130 Mulford Hall, Berkeley, California, 94720, USA*

16 ⁶ *Department of Earth Sciences, Utrecht University, Princetonlaan 8A, 3584 CB Utrecht, The*
17 *Netherlands*

18 *Corresponding author: kathrins@ldeo.columbia.edu

19 **Abstract**

20 Selenium (Se) isotope fractionation has been widely used for constraining redox conditions
21 and microbial processes in both modern and ancient environments, but our knowledge of the
22 controls on fractionation during microbial reduction of Se-oxyanions is based on a limited
23 number of studies. Here we complement and expand the currently available pure culture data
24 for Se isotope fractionation by investigating for the first time six phylogenetically and
25 physiologically non-respiring bacterial strains that reduce Se-oxyanions to elemental Se
26 [Se(0)]. Experiments were performed with either selenate [Se(VI)] or selenite [Se(IV)] at
27 lower, more environmentally-relevant concentrations (9 to 47 μM) than previously
28 investigated. *Enterobacter cloacae* SLD1a-1, *Desulfitobacterium chlororespirans* Co23 and
29 *Desulfitobacterium sp.* Viet-1 were incubated with Se(VI) and Se(IV). *Geobacter*
30 *sulfurreducens* PCA, *Anaeromyxobacter dehalogenans* FRC-W and *Shewanella sp.* (NR)
31 were examined for their ability reducing Se(IV) to Se(0). Our data confirm that microbial
32 reduction of both Se-oxyanions is accompanied by large kinetic isotopic fractionation
33 (reported as $^{82/76}\epsilon = 1000 * (^{82/76}\alpha - 1) \text{‰}$). Under our experimental conditions, microbial
34 reduction of Se(VI) shows consistently greater isotope fractionation ($\epsilon = -9.2\text{‰}$ to -11.8‰)
35 than reduction of Se(IV) ($\epsilon = -6.2$ to -7.8‰) confirming the difference in metabolic pathways
36 for the reduction of the two Se-oxyanions. For Se(VI), the inverse relationship between
37 normalized cell specific reduction rate (cSRR) and Se isotope fractionation suggests that the
38 kinetic isotope effect for Se(VI) reduction is governed by an enzymatically-specific pathway
39 related to the bacterial strain-specific physiology. In contrast, the lack of correlation between
40 normalized cSRR and isotope fractionation for Se(IV) reduction indicates a non-enzyme
41 specific pathway which is dominantly extracellular. Our study highlights the importance to
42 understand microbially-mediated Se isotope fractionation depending on Se species, and cell-
43 specific reduction rates before Se isotope ratios can become a fully applicable tool to
44 interpret Se isotopic changes in modern and ancient environments.

45

46 **1. Introduction**

47 Selenium (Se) isotope fractionation has been widely described in modern environments as
48 well as in ancient settings preserved in sedimentary rocks (Herbel et al., 2002; Mitchell et al.,
49 2012; Wen and Carignan, 2011; Wen et al., 2014; Schilling et al., 2015; Stüeken et al.,
50 2015a, b; Basu et al., 2016; Kipp et al., 2017). Selenium stable isotopes are particularly
51 sensitive to redox reactions, which determine chemical Se speciation in the environment. The
52 most mobile and bioavailable forms of Se are the water-soluble oxyanions selenate [Se(VI)]
53 and (hydro)selenite [Se(IV)]. Selenate is the dominant redox state in modern surface waters
54 (Martin et al., 2011) while Se(IV) is present in ocean surface water, but adsorbs strongly onto
55 iron, manganese and aluminum oxides (Parida et al., 1997; Peak and Sparks, 2002; Peak,
56 2006) as well as clays. Sparingly soluble elemental Se [Se(0)] and selenide [Se(-II)] are the
57 dominant redox states in anoxic environments. Typically, environmental Se concentrations
58 are at sub-micromolar levels (Conde and San Alaejos, 1997; Fordyce, 2013) but can locally
59 be elevated in sulfide ores and roll-front type uranium ores (Howard, 1977; Basu et al.,
60 2016), shales (Pogge von Strandmann et al., 2015; Stüeken et al., 2015a) or by anthropogenic
61 pollution. (*e.g.*, Presser and Ohlendorf, 1987; Dreher and Finkelman, 1992; Lemly, 2004;
62 Muscatello et al., 2008). Because the mobility and environmental impact of Se are
63 determined by its chemical speciation, it is important to understand the environmental
64 processes that control Se speciation and transitions between oxidation states.

65 Microbial reduction of Se-oxyanions is the primary set of reactions generating solid Se(0) in
66 natural settings. Both Se-oxyanions are energetically favourable electron acceptors because
67 the reduction of Se(IV) or Se(VI) can provide 90 to 150 times more free energy ' ΔG ' (- 8.9 to -
68 15.5 kcal mol⁻¹e⁻¹) for bacteria than the reduction of sulfate to sulfide (Stolz and Oremland,
69 1999). Bacteria able to reduce Se-oxyanions are phylogenetically diverse, have different
70 metabolic strategies, and have been isolated from both oxic and anoxic environments (*e.g.*,

71 Macy et al., 1993; Herbel et al., 2000; Stolz et al., 2006; Yee and Kobayashi, 2008; Pearce et
72 al., 2009). All microorganisms are facultative and it has been shown that non-specific
73 metabolic Se reduction can involve different enzyme systems, e.g. for reduction of nitrite,
74 nitrate, arsenate, sulfate and glutathione (*e.g.*, Switzer Blum et al., 1998; Sabaty et al., 2001;
75 Kessi and Hanselmann, 2004; Basaglia et al., 2007). Few Se(VI)-reducing bacteria have been
76 identified to catalyze Se(VI) reduction by the Se-specific enzyme selenate reductase
77 (Schröder et al. 1997; Bébien et al., 2002; Ridley et al., 2006, Theissen and Yee, 2014) and
78 only two bacterial strains (*Tetrathiobacter kashmirensis* and *Pseudomonas sp.*) have a
79 Se(IV)-specific enzyme (Hunter and Manter, 2008, 2009).

80 Limited published data on Se isotope fractionation during microbial Se reduction have
81 revealed large variations (Herbel et al., 2000; Ellis et al., 2003, Clark and Johnson, 2008). A
82 previous study with pure cultures (*Bacillus selenitireducens*, *Bacillus arsenicoselenatis* and
83 *Sulfurospirillum barnesii*) was restricted to dissimilatory Se-reducing bacteria grown with
84 very high millimolar levels of Se (10 – 20 mM) and with only lactate as electron donor at
85 high concentrations (10 – 40 mM). For these conditions, the reported Se isotope fractionation
86 varied greatly between -1.7 and -13.7‰ for the reduction of Se(IV) to Se(0) and -1.7 and -7.5
87 ‰ for reduction of Se(VI) to Se (IV) (Herbel et al., 2000). At contaminated sites, however,
88 Se concentrations are two to three orders of magnitude lower with Se concentration up to 150
89 μM (= 12,000 $\mu\text{g/L}$) in agricultural drainage and irrigation water (Deverel and Fujii, 1988;
90 Meseck and Cutter, 2011; Schilling et al., 2015) and up to 12 μM (= 955 $\mu\text{g/L}$) in waste
91 water from Se-bearing phosphorite mining (Mars and Crowley 2003; Stiling and Amacher,
92 2010). Even lower Se concentrations occur in modern ocean and aquifers with average values
93 of 0.002 μM and 0.5 μM Se, respectively (*e.g.*, Conde and San Alaejos, 1997; Pearce et al.,
94 2009; Basu et al., 2016).

95 Another study using sediments slurries reported Se isotopic fractionation by resident Se-
96 reducing microbial community between -8.3 and -8.6‰ for the reduction of Se(IV) to Se(0)
97 and -3.9 and -4.7‰ for the reduction of Se(VI) to Se(IV) (Ellis et al., 2003). Resident Se-
98 reducing microbial communities comprise diverse groups of bacteria with different metabolic
99 strategies. Although the magnitude of Se isotope fractionation by microbial reduction of Se-
100 oxyanions has been previously studied, the cause of such large variation in ϵ values and their
101 relevance for environmental settings remains unclear.

102 In this study, we extend the currently available experimental data by determining the isotopic
103 fractionation during microbial reduction of Se-oxyanions [Se(VI), Se(IV)] that includes
104 previously unexplored groups of mesophilic bacteria (Fig. 1), with the first results for
105 bacteria that perform non-catabolic reduction of Se-oxyanions. To investigate whether
106 different Se metabolic strategies affect the magnitude of isotopic fractionation, we selected
107 bacterial strains based on their ubiquitous distribution and their well-studied metabolisms.
108 For Se(VI) reduction, we conducted experiments with the Gram-negative bacterium
109 *Enterobacter cloacae* SLD1a-1, and the Gram-positive bacteria *Desulfitobacterium sp.* Viet-
110 1, and *Desulfitobacterium chlororespirans* Co23. For the reduction of Se(IV), we used
111 isolates of three Gram-negative bacteria namely *Geobacter sulfurreducens* PCA,
112 *Anaeromyxobacter dehalogenans* FRC-W and *Shewanella sp.* (NR) in addition to the three
113 Se(VI)-reducing bacterial strains. Studying pure bacterial cultures has the advantage to
114 eliminate any complexity from natural microbial communities such as competing strains with
115 possibly different reduction rates and to determine isotopic fractionation linked to a single
116 reduction mechanism. Further, we used lower electron acceptor and electron donor
117 concentrations compared to previous studies to achieve slow Se reduction rates as it is well
118 established that rapid reductions are transport limited and suppress the overall isotopic
119 fractionation (Clark and Johnson, 2010). These experimental conditions are very close to Se

120 concentrations reported for Se contaminated groundwater, soils, porewater (*i.e.*, Meseck and
121 Cutter, 2011; Stiling and Amacher, 2010; Schilling et al., 2015; Basu et al., 2016).

122 **2. Materials and Methods**

123 *2.1 Microbial culture*

124 The strains, *Desulfitobacterium sp.* Viet-1, *Desulfitobacterium chlororespirans* Co23,
125 *Geobacter sulfurreducens* PCA, *Aneromyxobacter dehalogenans* FRC-W and *Shewanella sp.*
126 (NR) (Table 1) were supplied by Sanford, and *Enterobacter cloacae* SLD1a-1 (Table 1) was
127 supplied by Pallud. For initial growth of bacterial cultures and for Se reduction experiments,
128 we used the mineral-salt medium described by He and Sanford (2002). One liter of test
129 medium was prepared with 10 mL buffer (12.5 g KH₂PO₄, 20.0 g K₂HPO₄ per liter), 10 mL
130 trace salt (1.17 g CaCl₂, 2.00 g MgCl₂ × 6H₂O, 0.70 g FeSO₄ × 7H₂O, 0.50 g Na₂SO₄ per
131 liter), 1 mL trace metals (0.05 g ZnCl₂, 0.5 g MnCl₂ × 4H₂O, 0.03 g CuCl₂ × 2H₂O, 0.05 g
132 CoCl₂ × 6H₂O, 0.05 g H₃BO₃, 0.05 g NiSO₄ × 6H₂O, 0.01 g Na₂MoO₄ × 2H₂O, 0.004 g
133 Na₂WO₄), 1 mL ammonium chloride, 1 mL selenium-tungsten and 0.84 g NaHCO₃. The
134 growth medium was supplemented with 0.03 g L-cysteine while the reductant L-cysteine was
135 omitted for the test medium used for Se batch experiments. Anaerobic condition in both
136 growth and test media was generated by boiling and degassing with N₂/CO₂ mix, the
137 subsequent transfer into 120 mL glass serum bottles sealed with butyl rubber stoppers, and
138 autoclaving at 121°C for 30 min.

139 In the growth medium, the bacterial strains *Desulfitobacterium chlororespirans* Co23 and
140 *Desulfitobacterium sp.* Viet-1 were initially grown under fermentative conditions using 10
141 mM pyruvate and *Enterobacter cloacae* SLD1a-1 using 2 mM glucose. *Shewanella sp.* (NR)
142 was incubated with 1 mM nitrate and 2.5 mM lactate. *Anaeromyxobacter dehalogenans* FRC-
143 W was incubated with 2.5 mM acetate and 1.25 mM nitrate. *Geobacter sulfurreducens* PCA
144 was grown with 3 mM acetate as electron donor and 10 mM fumarate as electron acceptor.

145 All anaerobic cultures were incubated at 30°C for 3 to 5 days to achieve high cell densities
146 ($\sim 10^{10}$ cells mL⁻¹) and complete consumption of the growth substrates.

147 2.2 Seleno-oxyanions reduction experiments

148 To test the reduction of Se-oxyanions, 10 mL of inoculum from the growth cultures,
149 corresponding to bacterial densities of 10^5 - 10^7 cells mL⁻¹ (Table 2) were transferred to the
150 test medium. The microbial cultures were amended with 10 to 47 μ M Se(VI) or Se(IV) as the
151 sole terminal electron acceptor. Depending on the bacterial strain, 500 μ M (2,000 and 10,000
152 μ M for *Geobacter sulfurreducens* PCA) acetate or lactate as electron donor was added to
153 each reactor (Table 1, 2). The experiments containing Se-oxyanions were conducted without
154 any chemical reducing agent to minimize any cell reproducibility and to avoid any abiotically
155 mediated Se reduction. The “no-cell” control experiments were carried out using identical
156 concentrations of electron donor and Se(VI) or Se(IV), but without any cell suspension. To
157 identify if viable cells were responsible for Se reduction, a “heat-killed cell” control of
158 *Desulfitobacterium chlororespirans* Co23 (autoclaved for 30 minutes) was inoculated with
159 18 μ M Se(VI) and 500 μ M lactate as electron donor. All cultures were incubated
160 anaerobically at 30°C under continuous shaking, and sampled at regular time intervals for
161 periods ranging from 60 to 800 hours, depending on the bacterial strains. Subsamples were
162 filtered through 0.2 μ m nylon filters.

163 2.3 Determination of cell-specific reduction rate (cSRR)

164 A 1 mL aliquot of each culture was sampled for cell counting at the beginning of the
165 experiment (t = 0). Cells were prefixed in 8% formaldehyde and stored at 4°C until analyzed.
166 Bacterial cells were stained with 1 μ L of the STYO bacterial stain and 10 μ L of microsphere
167 standard (bacteria counting kit, Invitrogen). The cell counting was performed by flow
168 cytometry analysis using a LSR II analyzer (BD Biosciences). The cell density was

169 determined from the cell-counts for a known number of microspheres in each sample. Culture
170 cell density values were used to calculate the initial cell density in the batch experiments and
171 to calculate the cell specific Se reduction rate (cSRR) using the following expression:

$$172 \quad \text{cSRR} = \Delta c / t_{1/2} \times d_0 \quad (\text{Eq. 1})$$

173 where Δc is the decrease in Se(VI) or Se(IV) concentration at the half-life $t_{1/2}$, and the initial
174 cell density d_0 . All cSRR values were normalized relative to the initial Se concentrations.

175 *2.4 Transmission electron microscopy (TEM)*

176 Microbial cultures of *Enterobacter cloacae* SLD1a-1 were incubated with Se(VI) or Se(IV)
177 for 24 hours. Afterwards the bacterial cells were pre-concentrated by centrifugation and fixed
178 with 2% glutaraldehyde in a 0.04 M phosphate buffer. After the second cell fixation using 1%
179 osmium tetroxide, the samples were dehydrated with different concentrated ethanol
180 solutions and embedded in resin. After sectioning of the bacterial cells, micrographs were
181 taken with a Technai 12 transmission electron microscope (University of California,
182 Berkeley).

183 *2.5 Se isotope and concentration analysis*

184 Initially, the concentrations of dissolved Se species [Se(VI) and/or Se(IV)] were measured
185 using mass ^{78}Se by hydride generation-inductively coupled plasma-mass spectrometry (ICP-
186 MS). Prior to measurement, Se(VI) was converted to Se(IV) by heating at 105°C degrees for
187 60 minutes in a 5 M HCl matrix. The reported Se concentrations were calculated using an
188 isotope dilution double-spike method by adding $^{74}\text{Se} + ^{77}\text{Se}$ double spike of known isotope
189 ratio and concentration to the sample with unknown Se concentration (*e.g.*, Heumann, 1992).
190 We also used double spike isotope technique with an approximate sample spike proportion of
191 2 to correct for isotopic fractionation during sample purification and instrumental mass bias
192 during the isotope measurement.

193 Selenium species separation from matrix solutes was performed using 1 mL AG1-X8 anion-
194 exchange resin (Eichrom). Prior to anion-exchange, all subsamples of Se(IV) were oxidized
195 to Se(VI) with a 20 mM solution of the strong oxidizer potassium persulfate (Schilling et al.,
196 2014, 2015) prior to heating at 90°C for 1h. The sample purification procedure (including an
197 oxidation step for Se(IV) and chromatographic separation for all samples) resulted in
198 recoveries of >90%.

199 Selenium isotope ratios were measured using a Nu Plasma high resolution multiple collector-
200 ICP-MS, connected to a custom-built hydride generation system described in previous studies
201 (e.g., Clark and Johnson, 2008; Mitchell et al. 2012; Zhu et al., 2014; Schilling et al., 2015;
202 Mitchell et al., 2016). All $^{82}\text{Se}/^{76}\text{Se}$ ratios are reported as δ notation relative to the NIST SRM
203 3149 inter-laboratory standard:

$$204 \quad \delta = \frac{\text{Sample} / \text{Standard} - 1}{\text{Standard} / \text{Standard} - 1} \quad (\text{Eq. 2})$$

205 Blank solutions processed through the same sample purification procedure contained an
206 average of 4.4 ± 2.9 ng Se (n=12), less than 0.7% of the total sample. The uncertainty on
207 $\delta^{82/76}\text{Se}$ was estimated by calculating the root mean square difference (RMS) for samples
208 prepared and analyzed in duplicate (n = 25). The in-house standard MH-495 was measured
209 with an average value of $-3.35 \pm 0.1\%$ (2σ , n = 12) relative to SRM-3149 within excellent
210 agreement of previously reported values (Carignan and Wen, 2007; Zhu et al., 2008).
211 Average external $^{82/76}\text{Se}$ precision was $\pm 0.16\%$ based on repeated analysis of SRM-3149
212 standards (n = 145) over two years. The external reproducibility for $^{82/76}\text{Se}$ of the samples,
213 determined as twice root mean square, was $\pm 0.17\%$ (n = 25) across a range of $\delta^{82/76}\text{Se}$ values
214 between -0.3‰ and +29.3‰.

215 *2.6 Determination of the magnitude of isotopic fractionation (ϵ)*

216 As all experiments were conducted in sealed batch reactors, the experiments were assumed to
217 follow closed system behavior. Positive $\delta^{82/76}\text{Se}$ values of the remaining, unreacted Se thus
218 indicate enrichment in heavy isotopes relative to the standard, whilst negative values
219 represent depletion of heavy isotopes. Changes in $\delta^{82/76}\text{Se}$ can be directly related to the extent
220 of Se(VI) or Se(IV) reduction. The magnitude of Se isotope fractionation was determined for
221 each experiment by fitting the measured $\delta^{82/76}\text{Se}$ values to Rayleigh distillation models
222 following the method described by Scott et al. (2004):

223
$$\delta^{82/76}\text{Se} = \left(\frac{c(t)}{c_0} \right)^{\alpha} - 1 \quad \text{---} \quad \text{(Eq.3)}$$

224 where $c(t)$ and $\delta(t)$ are the concentration and the isotopic composition of the remaining
225 reactant (Se(VI) or Se(IV)) in solution as a function of reaction time. The fractionation factor
226 (α) is defined as defined as $\alpha = R_{\text{product}}/R_{\text{reactant}}$, where R is the measured $^{82}\text{Se}/^{76}\text{Se}$, and often
227 expressed in terms of ε (a per mil quantity) as

228
$$\varepsilon = (\alpha - 1) \times 1000 \quad \text{(Eq. 4)}$$

229 The magnitude of isotopic fractionation, ε , was calculated from the corresponding slope from
230 the linear regression of $\ln(\delta^{82}\text{Se} + 1000)$ versus $\ln(c(t)/c_0)$.

231 2.7 Statistical analysis

232 One-way analysis of variance (ANOVA) with Tukey-HSD test ($\alpha = 0.05$) was used to
233 evaluate the potential difference in the magnitude of Se isotope fractionation (ε) between
234 Se(IV) or Se(VI) reduction by the different bacterial strains and among the different bacterial
235 strains. The statistical analyses were performed using JMP software 13.1.0. with a statistical
236 probability of $P < 0.05$.

237 3. Results

238 3.1 Microbial reduction of Se(VI)

239 Figure 2 shows Se(VI) removal over time during anaerobic microbial Se(VI)-reduction
240 experiments by three bacterial strains (*Enterobacter cloacae* SLD1a-1, *Desulfitobacterium*
241 *chlororespirans* Co23, *Desulfitobacterium sp.* Viet-1). In the presence of Se(VI)-reducing
242 bacteria, the decrease in Se(VI) concentration ranged between 51% to 99% relative to the
243 initial Se(VI) concentrations in the batch reactors. In all experiments, the decrease in Se(VI)
244 concentration with time follows a first-order kinetics except for the latest sampling points. A
245 single first-order rate constant reasonably fit all data from each experiment. The heat-killed
246 control with bacterial cells from *Desulfitobacterium chlororespirans* Co23 did not show any
247 measurable Se(VI) removal after ca. 4 days of incubation (Figure 2A). We observed in the
248 batch reactors an initial increase in Se(IV) resulting from the reduction of Se(VI), followed
249 by Se(IV) reduction to Se(0) (Table A1).

250 In all Se(VI) experiments, an enrichment of ^{82}Se occurred in the remaining unreacted Se(VI)
251 with progressive Se(VI) reduction (Figure 3). The largest $\delta^{82/76}\text{Se}$ value of +38.6‰ was
252 observed at 99% reduction of Se(VI) for the experiment with *Desulfitobacterium sp.* Viet-1
253 (Figure 3C). The $\delta^{82/76}\text{Se}$ values for the intermediate Se(IV) varied between -9.6‰ for 1.5%
254 Se(IV) and 16.6‰ for 15% Se(IV) relative to the initial Se(VI) concentration (9 μM) (Table
255 A1). The magnitudes of Se isotopic fractionation (ϵ) for microbial Se(VI) reduction, obtained
256 by fitting $\delta^{82/76}\text{Se}$ data to Eq. 3, are illustrated in Figure 3 and reported in Table 3. Among the
257 three Se(VI)-reducing pure bacterial cultures, the ϵ values varied between -9.2‰ and -11.8‰
258 with a mean value of $-10.6 \pm 1.3\text{‰}$. The ϵ values did not deviate in duplicate reactors within
259 a 2σ uncertainty limit. The initial cell densities varied by two orders of magnitude in the
260 Se(VI) incubation with the highest cell density of $1.9 \times 10^8 \text{ cell ml}^{-1}$ for the batch of
261 *Enterobacter cloacae* SLD1-1a. The normalized cSRR ranged from 0.11×10^{-17} to 1.30×10^{-17}
262 $\text{mol Se(VI) cell}^{-1} \text{ d}^{-1}$ (Table 2). We observed a strong inverse relationship ($r^2 = 0.91$) between

263 normalized cSRR and ϵ for Se(VI) reduction with decreasing ϵ values for increasing values of
264 cSRR (Figure 4A).

265 Transmission electron microscope images of a washed cell suspension of *Enterobacter*
266 *cloacae* SLD1a-1 after the reduction of Se(VI) showed intracellular Se(0) precipitates (Figure
267 5A). The particle sizes were spherical, $<0.2 \mu\text{m}$ in diameter and located in the periplasmic
268 space.

269 3.2. Microbial reduction of Se(IV)

270 Anoxic batch incubations of six Se-reducing bacterial strains with Se(IV) showed a decrease
271 in Se(IV) concentration as a function of time (Figure 6 and Table A2). The Se(IV) removal
272 ranged between 56% to 92% over a period of 0.4 to 6.1 days. The no-cell control experiments
273 did not show any change in Se(IV) concentrations with time. In each experiment, a first order
274 kinetic model with a single rate constant fits all Se(IV) concentration data. The time interval
275 for 50% removal of the initial Se(IV) concentration varied from 0.42 to 3.1 days. *Geobacter*
276 *sulfurreducens* PCA assayed with varying electron donor concentrations (2,000 to 10,000
277 μM) exhibited an approximately 50% Se(IV) removal after similar time periods ($t_{1/2}$ 0.49 to
278 0.66 days).

279 The initial cell densities varied by approximately two-orders of magnitudes depending on the
280 volume of inoculum. The highest cell density was found for the Se(IV) batch of
281 *Anaeromyxobacter dehalogenans* FRC-W ($1.3 \times 10^8 \text{ cell ml}^{-1}$) and the lowest for
282 *Enterobacter cloacae* SLD1a-1 ($8.8 \times 10^6 \text{ cell ml}^{-1}$). The calculated cell-specific reduction rate
283 ranged from 0.28 to $5.7 \times 10^{-17} \text{ mol cell}^{-1} \text{ d}^{-1}$ with no correlation between normalized cSRR
284 and ϵ values ($r^2 = 0.13$; Figure 3B). We observed no correlation between normalized cSRR
285 and ϵ for Se(IV) reduction (Figure 4B).

286 While the Se(IV) concentration in the batch reactors decreased, $\delta^{82/76}\text{Se}$ progressively
287 increased with time (Figure 7) relative to the starting Se(IV). The duplicate batch reactors

288 showed similar ϵ values within the 2σ uncertainty level of $\pm 0.12\text{‰}$ to $\pm 0.43\text{‰}$. (Table 3). The
289 largest $\delta^{82/76}\text{Se}$ value of $+15.7\text{‰}$ was observed for *Shewanella sp.* (NR) after 91% Se(IV)
290 removal. The ϵ values for Se(IV) reduction span a narrow range of -6.2‰ to -7.8‰ with a
291 mean value of $-7.0 \pm 0.6\text{‰}$. We observed no significant difference in ϵ values among the six
292 different bacterial strains ($p = 0.376$; Figure 7).

293 Transmission electron microscope images of *Enterobacter cloacae* SLD1a-1 incubated with
294 Se(IV) showed exogenous precipitates, presumably Se(0) (Figure 5A) which are smaller than
295 the intracellular Se(0) particles observed as a product of Se(VI) reduction (Figure 5B).

296 **4. Discussion**

297 Our results demonstrate that the magnitude of Se isotope fractionation by microbial reduction
298 of Se-oxyanions depends mainly on two factors (1) growth conditions and (2) the Se-
299 reduction by cometabolic or Se-respiring pathway. Below we discuss variation in Se isotope
300 fractionation based on these two factors, specifically in the context of previous studies.
301 Differences in the magnitude of Se isotope fractionation in our study compared to the
302 previous studies (Herbel et al., 2000; Ellis et al., 2003; Clark and Johnson, 2008) is attributed
303 to differences in the experimental approach and selection of bacterial strains.

304 *4.1. Effect of experimental conditions on ϵ*

305 In the following section we discuss the reasons behind differences in the magnitude of Se
306 isotope fractionation between our study and previous studies (Herbel et al., 2000; Ellis et al.,
307 2003; Clark and Johnson, 2008).

308 *4.1.1 Comparison to pure culture studies*

309 Environmentally-relevant conditions, more specifically much lower Se substrate
310 concentrations, result in a narrower-range Se isotope fractionation factors for the reduction of
311 both Se(VI) and Se(IV) compared to previously published values obtained for *Bacillus*

312 *selenitireducens*, *Bacillus arsenicoselenatis* and *Sulfurospirillum barnesii* (Herbel et al.
313 2000). Indeed, Herbel et al. (2000) experiments were conducted under highly optimum
314 growth conditions for anaerobic Se respiration *i.e.*, using high initial Se-oxyanion
315 concentrations (10 - 20 mM) and high carbon concentrations (10 - 40 mM). This led to fast
316 reduction rates and 100-fold increase in cell density during the experiment, which might
317 explain the large span in isotopic fractionation they observed for Se(VI) reduction ($\epsilon = -1.7$ to
318 -7.5% ; Herbel et al., 2000). In addition, Se reduction rates in the previous study were one-
319 order of magnitude (10^{-16} mol cell⁻¹ d⁻¹) higher than the cSRRs observed in our experiments
320 (10^{-17} mol cell⁻¹ d⁻¹). In contrast to the large increase in cell density in the experiment by
321 Herbel et al (2000), natural microbial consortia generally maintain a rather steady state
322 population where cell decay balances cell growth (Brock, 1971). The more uniform ϵ values
323 in our study correspond to minor cell growth or decay evident from single first-order rate
324 constants fitting the time series from each experiment and thus more consistent cSRRs
325 throughout the experiment. Moreover, three-orders of magnitude lower initial Se-oxyanions
326 concentrations, together with 20 times lower carbon concentrations as electron donor (10 mM
327 vs. 0.5 mM), led to significantly larger ϵ values ($\epsilon = -9.2\%$ to -11.8%). Likewise, our data on
328 microbial Se(IV) reduction result in an overall narrow distribution of ϵ values ($\epsilon_{\text{mean}} = -7 \pm$
329 0.6%) compared to the previous study ($\epsilon = -1.7$ to -13.7% ; Herbel et al., 2000). This narrow
330 range of ϵ values is likely when the tested strains are not actively respiring Se. Instead, the
331 reduction of Se-oxyanions is a response to cope with the element's toxicity. Lower initial
332 Se(IV) concentration also affect the results in two different ways by producing lower
333 reduction rates and lower Se concentrations are less toxic for the cells and thus maintains the
334 cell viability.

335 Whether bacteria reduce Se as respiration pathway (Herbel et al., 2000) or as a cometabolic
336 pathway determines the magnitude of isotope fractionation. All bacterial strains (*Bacillus*

337 *selenitireducens*, *Bacillus arsenicoselenatis* and *Sulfurospirillum barnesii*) used in Herbel et
338 al. (2000) are capable of actively metabolizing Se oxyanions. This means that the bacteria are
339 able to harness the energy derived from coupling reduction of Se(VI)/Se(IV) and oxidation of
340 lactate to synthesize biomass. This leads to bacterial growth (increase of cell density by about
341 two orders of magnitude) during the experiments which changes the cSRR and thus affects
342 the ϵ values. For example, isotope fractionation by *Bacillus selenitireducens* varied between -
343 2.6 and -13.7‰ (Herbel et al., 2000). This also explains why the relationship between cSRR
344 vs. ϵ breaks down for Se-respiring bacteria. Further, both Se(VI)-respiring bacterial strains,
345 *Bacillus arsenicoselenatis* and *Sulfurospirillum barnesii*, only reduce a very small amount of
346 Se(IV) to Se(0) (Herbel et al., 2000), while our tested bacterial strains reduce Se(VI) all to
347 Se(0) (Table A1).

348 Although the tested Se-reducers are not confined to any particular group of bacteria (Figure
349 1), we demonstrate that not the phylogenetic differences but the metabolic mechanisms
350 control Se isotope fractionation. There is no systematic difference in ϵ between the tested
351 non-respiring Gram-positive (*Desulfitobacteria*) and Gram-negative bacteria (*Enterobacter*
352 *cloacae* SLD1a-1). Gram-negative bacteria possess two membranes separated by the
353 periplasmic space. The selenate reductase of Gram-negative bacterium *Enterobacter cloacae*
354 SLD1a-1 is a membrane-bound enzyme situated in the cytoplasmic (inner) membrane
355 (Schröder et al., 1997; Bébien et al., 2002; Ma et al., 2009). The location for the Se(VI)-
356 reducing enzymes of *Desulfitobacterium chlororespirans* Co23 and *Desulfitobacterium sp.*
357 Viet-1 are not known but are probably also membrane-bound as described for other Se(VI)-
358 reducing Gram positive bacteria (Kuroda et al., 2011). Hence, the diffusive transport across
359 the outer membrane for Gram-negative bacteria seems not to affect the reaction rate and Se
360 isotope fractionation for Se(VI) reduction.

361 In bacterial strains with no Se-specific enzymatic pathway, the reduction is carried out by
362 various enzyme systems, e.g. nitrite reductase, nitrate reductase, arsenate and sulfate
363 reductases, or the reduction of Se(IV) by glutathione (*e.g.*, Tomei et al., 1995; Switzer Blum
364 et al., 1998; Sabaty et al., 2001; Kessi and Hanselmann, 2004; Basaglia et al., 2007;
365 Nancharaiah and Lens, 2015). These enzyme systems have mainly a detoxifying function and
366 the energy released by the redox reaction is not generally utilized to synthesize biomass.
367 Therefore, we assume that the obtained isotope fractionation factors can be extrapolated to a
368 much wider group of microorganisms because the studied pure cultures include bacteria with
369 different cell membranes (Gram positive and Gram negative), different enzymes in the
370 electron transfer chain (*e.g.*, selenate reductase for *Enterobacter cloacae*) and carbon
371 substrates (acetate and lactate) but show nearly identical isotope fractionations for the
372 reduction of the respective Se-oxyanion.

373 4.1.2 Comparison to natural microbial consortia in sediment slurries and cores

374 Our pure culture microbial Se(VI) reduction experiments induced significantly larger Se
375 isotope fractionation than experiments with sediment slurries and sediment cores involving
376 complex microbial communities (Ellis et al., 2003; Clark and Johnson, 2008). Here reported ϵ
377 values relate to suspensions of free-living cells with maximized mass transfer and
378 accessibility of Se-oxyanions for each bacterial cell. Mass transfer limitation in sediment
379 slurries and cores is expected to decrease the exchange between Se(VI) in solution and the
380 particle-bound bacteria. This in turn should reduce selectivity for an isotopologue (heavy vs.
381 light). Generally, mass transfer is faster for the isotopically light ^{76}Se -oxyanions than for the
382 isotopically heavy ^{82}Se -oxyanions. If the probability for Se(VI) selectivity of an isotopologue
383 is limited for the particle-bound bacteria the mass transfer affects the Se isotope fractionation.
384 This presumably explains the relatively small Se isotope fractionation observed in sediment
385 slurries (Ellis et al., 2003) where the contact between bacteria and Se-oxyanions in solution is

386 limited but still higher than for sediment cores (Clark and Johnson, 2008). Selenium isotope
387 signals in sediments controlled by the diffusion of Se from the overlying water have the
388 highest mass transfer limitation determined by incomplete solution exchange at the water-
389 sediment interface and the lowest Se isotope fractionation of 0.4‰ for microbial Se
390 reduction. In contrast, pure cultures in our study are more selective to a particular Se
391 isotopologue (heavy vs. light) as they are not particle-bound. However even if in porewaters,
392 diffusion limitation yields a smaller Se isotope fractionation the reduction of Se(VI) and
393 Se(IV) are still detectable because the shift in δ values from the initial value is significant.

394 4.2. Effect of metabolic pathway on Se isotope fractionation

395 Reduction of Se-oxyanions occurs intracellularly in the periplasmic space for Se(VI) (*i.e.*,
396 Ridley et al., 2006; Nancharaiah and Lens, 2015) or extracellularly for Se(IV) (*e.g.*, Pearce et
397 al., 2009; Nancharaiah and Lens, 2015). Our data and the pure culture study by Herbel et al.,
398 (2000) confirm that the pathways for reduction of Se(VI) or Se(IV) determine the Se isotope
399 fractionation. Microbial Se(VI) reduction induces significantly larger fractionation than
400 Se(IV) reduction for the six tested bacterial strains ($p > 0.01$).

401 4.2.1 Intracellular Se(VI) reduction

402 The reduction Se(VI) to Se(0) is a sequential two-step reaction which leads to significantly
403 larger fractionation than Se(IV) reduction for the tested bacterial strains ($p > 0.01$). The
404 reduction of Se(VI) to Se(IV) *via* two electron transfer is followed by a four electron transfer
405 to form Se(0). Heat-killed control experiments with *Desulfitobacterium chlororespirans*
406 Co23, which did not show Se(VI) reduction and any concomitant Se isotopic fractionation,
407 confirms that Se(VI) reduction is enzymatically-mediated by viable cells. Correlation
408 between normalized cSRR and ϵ for Se(VI) reduction indicates that the rate of electron
409 transfer depends on the abundance of bacteria and their enzymes (*e.g.*, selenate reductase)

410 (Yee and Kobayashi, 2008). Mechanistically, diffusion transport brings Se(VI) to the
411 reduction site of the bacterial cell where Se(VI) is then reduced intracellularly. As diffusive
412 transport of Se(VI) does not involve changes in coordination of oxygen around Se, any
413 discrimination between the isotopologes in the Se-oxyanions will be minor compared to
414 enzymatic reduction. If the reduction rate of Se(VI) at these reduction sites is very slow either
415 due low abundances of bacteria and their enzymes it is expected that ϵ reaches a maximum
416 value. Future studies can help determining the maximum value as well as the more in-depth
417 understanding of the relevant enzymes involved in the cometabolic Se(VI) reduction and the
418 related Se isotope fractionation.

419 4.2.2 Extracellular Se(IV) reduction.

420 The four electron transfer by only one reduction step for Se(IV) explains the smaller Se
421 isotope fractionation compared to the reduction of Se(VI). Electron transfer for the reduction
422 of Se(IV) is driven by either an exogenous electron shuttle, extracellular proteins or possibly
423 pili structures (Pearce et al., 2009). This also explains why the magnitude of Se isotope
424 fractionation does not correlate with normalized cSRRs (Figure 4C) because an exogenous
425 electron transfer does not require a direct contact between the bacterial cell and the substrate
426 via a specific enzyme. Such extracellular reaction is also most likely decoupled from electron
427 donor oxidation, so that different donor types or concentrations do not affect the isotope
428 fractionation factor. This is clearly shown for the experiments with *Geobacter sulfurreducens*
429 PCA, known for reducing Se(IV) extracellularly by outer membrane cytochromes (Pearce et
430 al., 2009). Varying concentrations of electron donor (500 to 10,000 μM) have no effect on ϵ
431 values (Table 3) for Se(IV) reduction by *Geobacter sulfurreducens* PCA. This is consistent
432 with the observation for microbial Cr(VI) reduction where an extracellular Cr reduction
433 pathway results in uniform Cr isotope fractionation at different electron donor concentrations
434 (*i.e.*, Sikora et al., 2008; Basu et al., 2014; Zhang et al., 2019). Further, the extracellular

435 reduction pathway for Se(IV) is not impacted by mass transfer limitation of Se(IV) to the
436 bacterial cell and this explains the relatively good agreement for isotope fractionation
437 between sediment slurry experiments for particle-bound natural microbial consortia ($\epsilon = -$
438 8.4‰; Ellis et al., 2003) and our pure culture study with free-living cells ($\epsilon = -6.2$ to -7.8%).

439 **5. Implications**

440 Given the distinctive amounts of Se isotope fractionation for microbial reduction of the two
441 Se-oxyanions, Se isotope ratios can, in principle, shed light on the processing of Se-
442 oxyanions in both modern and ancient environments.

443 *5.1. Modern environments.*

444 Selenium stable isotope ratios have been previously used as indicators for Se sources and
445 cycling in aquifers, lakes, soils and sediments (Clark and Johnson 2010; Schilling et al.,
446 2015; Basu et al., 2016). Microbial reduction of Se reduces the mobility of Se from soluble
447 poorly adsorbed Se(VI), to soluble strongly adsorbed Se(IV), to solid Se(0).

448 Our ϵ values can be understood as reference values to estimate the extent of Se
449 reduction for bacterial groups most commonly found in the environment. A clear indicator of
450 the reduction of Se(VI) to Se(IV) is the enrichment of ^{82}Se in Se(VI) or Se(IV) in
451 groundwater or porewater while the reduced Se species in sediments and soils is enriched in
452 ^{76}Se . If microbial Se reduction is the dominant reaction mechanism in nature, this should be
453 reflected by shifts in $\delta^{82/76}\text{Se}$ ratios according to the aqueous speciation of Se and the ϵ for
454 that particular reaction.

455 In groundwater systems, we can infer the ϵ for Se removal mechanism from $\delta^{82/76}\text{Se}$ of
456 Se(VI) and Se(IV) measured in the same sample (Schilling et al., 2015; Basu et al., 2016).
457 The Microbial reduction of Se-oxyanions in a groundwater plume moving through a redox
458 gradient will fractionate $\delta^{82/76}\text{Se}$ of both the reactant and the product. This fractionation

459 combined with the reactive transport of Se should lead to a systematic pattern of $\delta^{82/76}\text{Se}$
460 induced by a distillation effect in the groundwater. With progressive reduction along the flow
461 path, Se-oxyanions will become isotopically heavy. For instance, Basu et al. (2016) observed
462 increasing $\delta^{82/76}\text{Se}$ with decreasing Se(VI) concentrations in an aquifer along the redox
463 gradient at an *in-situ* recovery mining site. However, along the flow path of groundwater the
464 rate of microbial Se reduction may vary depending on the organic carbon content of the
465 aquifer, and the bacterial population density. This variation in the Se reduction rates can
466 systematically affect the ϵ , which is determined by the difference in $\delta^{82/76}\text{Se}$ between Se(VI)
467 and Se(IV) of the same sample.

468 The dependence of ϵ on the Se(VI) reduction rate has important implications for predicting
469 Se removal/accumulation patterns in modern settings based on Se isotope ratios. Our
470 experimental results suggest a higher ϵ at low Se(VI) reduction rates generally found in
471 terrestrial sediments with low organic carbon. In contrast, lower ϵ is expected in geochemical
472 settings with high Se(VI) reduction rate commonly found after organic carbon amendment
473 (*i.e.*, acetate) at active bioremediation sites. Our results suggest that the ϵ inferred from water
474 samples may be used to estimate the Se(VI) reduction rate, which is difficult to determine
475 accurately in open systems. Similarly, if the Se(VI) reduction rate is known, an appropriate
476 ϵ can be determined for calculating the extent of remediation for active remediation sites
477 using rate- ϵ relationship. Therefore, any quantitative interpretation of the groundwater Se
478 isotope ratios is predicated on the knowledge of the size of the intrinsic ϵ and the factors that
479 control ϵ at a geochemical setting.

480 Sedimentary Se isotope ratios may provide a complimentary view of the relationship
481 between reduction rate of Se oxyanions and ϵ . The $\delta^{82/76}\text{Se}$ values of different Se soil pools in
482 agricultural seleniferous soils vary up to 13‰ (Schilling et al., 2015). The isotopically heavy

483 adsorbed Se(IV) in the agricultural seleniferous soils suggest Se isotope fractionation by
484 microbial reduction of Se(VI) in irrigation water prior to scavenging of the reaction product
485 Se(IV) by reactive minerals in the soil. Therefore, our laboratory-derived ϵ values for
486 microbial reduction are essential to quantitative determination of the extent of microbial
487 reduction in the field. Nevertheless, site-specific ϵ values should still be obtained from
488 experiments using the resident Se-reducing microbial community

489

490 5.2. Ancient environments

491 The Se isotope signature preserved in rocks and sediments can be used to constrain the
492 evolution of the biosphere and redox conditions in near surface environments through time
493 (Wen and Carignan, 2011; Mitchell et al., 2012, 2016; Wen et al., 2014; Stüeken et al.,
494 2015a, b; Kipp et al., 2017). However, interpreting Se isotope signature preserved in rocks
495 and sediments is still difficult as (1) bulk rock Se isotope data mask the variability in Se
496 isotope ratio of various Se phases (*i.e.*, organically-bound, pyritic, adsorbed) in the rocks and
497 (2) the effects of local versus global controls on Se cycling due to the short oceanic residence
498 time (10^3 years) of Se species and their low concentrations ($<1\text{nM}$). Therefore, the
499 application of Se isotopes as a paleoredox proxy relies on experimentally determined ϵ values
500 for microbial reduction of Se-oxyanions. High-resolution isotope analyses with an analytical
501 precision of 0.2‰ allows to resolve different reaction pathways and fingerprint Se sources
502 preserved within the rock record.

503 Selenium isotope signature in bulk shales range between -1.5 and +2.2‰ over geological
504 time (Wen and Carignan, 2011; Mitchell et al., 2012; Pogge von Strandmann et al., 2014;
505 Stüeken et al., 2015a, b; Mitchell et al., 2016). The sequestration of isotopically light Se has
506 been reported for shale deposits (Wen and Carignan, 2011; Mitchell et al., 2012; Pogge von
507 Strandmann et al., 2014; Stüeken et al., 2015a, b) suggesting the partial reduction of Se-

508 oxyanions in suboxic basins. Our results suggest a lower ϵ during very rapid removal of
509 Se(VI), the dominant Se species in the ocean (Conde and Alaejos, 1997), during anoxia
510 which is consistent with small changes in $\delta^{82/76}\text{Se}$ in the black shales. However, it is
511 necessary to extract phase-specific Se (*i.e.*, adsorbed, organic, pyritic) from rocks and
512 sediments and determine their Se isotope compositions to disentangle microbial reduction of
513 Se-oxyanions from other reaction pathways (*i.e.*, adsorption and assimilation). It should be
514 noted that muting of ϵ values are expected in semi-closed or open flow through systems
515 (Shrimpton et al., 2018) like microbial Se reduction in porewater in ancient oceans compared
516 to ϵ values typically observed during Rayleigh distillation in a closed system.

517 In our study, we demonstrate that decreasing microbial activity results in smaller
518 cSRR, which causes larger Se isotope fractionation and this could ultimately be reflected in
519 lighter Se isotopic signature in sedimentary Se reservoirs. Despite uncertainties about the Se
520 concentrations and its speciation in ancient oceans, our results imply a systematic relationship
521 between the rate of Se reduction and the observed Se isotope fractionation which must be
522 considered when interpreting $\delta^{82/76}\text{Se}$ signatures. This relationship can be of great importance
523 because Se reduction rates may be derived from Se isotope signature preserved in the rock
524 record. Thus, the Se isotope signatures recorded in ancient sediments should be re-examined
525 given the influence of Se(VI) reduction rate on the magnitude of Se isotope fractionation.

526 Future studies should be designed to constrain Se isotope fractionation at microbial Se
527 reduction rates relevant to ancient marine conditions and reconstruct $\delta^{82/76}\text{Se}$ ratios imprinted
528 in the rock record. Additionally, phase-specific Se isotope analysis for rocks and sediments,
529 and quantitative modeling approaches can help to provide further insight into the microbial
530 Se cycling in the ancient ocean.

531 **6. Summary and Conclusions**

532 This study provides the first insights on the variation of Se isotope fractionation for non-
533 respiring Se reduction by six different bacterial strains (*Geobacter sulfurreducens* PCA,
534 *Anaeromyxobacter dehalogenans* FRC-W, *Shewanella* sp. (NR), *Enterobacter cloacae*
535 SLDa1-1, *Desulfitobacterium chlororespirans* Co23 and *Desulfitobacterium* sp. Viet-1). We
536 demonstrate that under environmentally-relevant experimental conditions (e.g., <42 μM Se;
537 500 μM electron donor), Se isotope fractionation factors reveal a relatively narrow range for
538 both Se(VI) and Se(IV) reduction with consistently larger Se isotope fractionation for Se(VI)
539 ($\epsilon_{\text{mean}} = -10.6 \pm 1.3\text{‰}$) than for Se(IV) reduction ($\epsilon_{\text{mean}} = -7 \pm 0.6\text{‰}$). Based on the present
540 and previous studies on microbial reduction of Se-oxyanions, we conclude that Se isotopic
541 fractionation during microbial reduction is controlled by the co-metabolic reaction
542 pathway(s).

543 **Acknowledgement**

544 The authors wish to thank Linden Schneider for helping with the experiment. This study was
545 financially supported by the Netherlands Organisation for Scientific Research grant number
546 820.02.007.

547

548 **References**

- 549 Basu A., Schilling K., Brown S.T., Johnson T.M., Christensen J., Hartmann M., Reimus P.,
550 Heikoop J., WoldeGabriel G., DePaolo D.J. (2016) Selenium isotope ratios
551 groundwater redox indicators: Detecting natural attenuation of Se at an In Situ
552 Recovery U mine *Environ. Sci. Technol.* **50**, 10833-10842.
- 553 Basu A., Johnson T.M., Sanford R.A. (2014) Cr isotope fractionation factors for Cr(VI)
554 reduction by a metabolically diverse group bacteria. *Geochim. Cosmochim. Acta* **142**,
555 349-361.
- 556 Basaglia M. Toffanin A., Baldan E. Bottegal M., Shapleigh J.P., Casella S. (2007) Selenite-
557 reducing capacity of the cooper-containing nitrite reductase of *Rhizobium sullae*.
558 *FEMS Microbiol. Lett.* **269**, 124-130.
- 559 Bébien M., Kirsch J., Mejean V., Vermeglio A. (2002) Involvement of a putative
560 molybdenum enzyme in the reduction of selenate by *Escherichia coli*. *Microbiol.* 148:
561 3865-3872.
- 562 Brock T.D. (1971) Microbial growth rates in nature. *Bacteriol. Rev.* 35: 39-58.
- 563 Carignan J., Wen H. (2007) Scaling NIST SRM3149 for Se isotope analysis and isotopic
564 variations of natural samples. *Chem. Geol.* **242**, 347-350.
- 565 Clark S.K., Johnson T.M. (2008) Effective isotopic fractionation factors for solute removal
566 by reactive sediments: A laboratory microcosm and slurry study. *Environ. Sci.*
567 *Technol.* **42**, 7850-7855.
- 568 Clark S.K., Johnson T.M. (2010) Selenium stable isotope investigation into selenium
569 biogeochemical cycling in a lacustrine environment. Sweitzer Lake, Colorado. *J.*
570 *Environ. Qual.* **39**, 2200-2210.
- 571 Conde J.E., San Alaejos M. (1997) Selenium concentration in natural and environmental
572 waters. *Chem. Rev.* 97: 1979-2003.
- 573 Deverel S.J. and Fujii R. (1988) Processes affecting the distribution of selenium in shallow
574 groundwater of agricultural areas, western San Joaquin Valley, California. *Water*
575 *Resour. Res.* **24**, 516-524.
- 576 Dreher G.B., Finkelman R.B. (1992) Selenium mobilization in a surface coal mine, Powder
577 River Basin, Wyoming, USA. *Environ. Geol. Water Sci.* **19**, 155-167.
- 578 Ellis A.S., Johnson T.M., Bullen T.D., Herbel M.J. (2003) Stable isotope fractionation of
579 selenium by natural microbial consortia. *Chem. Geol.* **195**, 119-129.
- 580 Fordyce, F.M. 2013. Selenium deficiency and toxicity in the environment. IN: Essentials of
581 Medical Geology, O. Selinus (eds.) British Geol. Survey. 375-416.
- 582 He Q., Sanford R.A. (2002) Induction characteristics of reductive dehalogenation in the
583 ortho-halophenol-respiring bacterium, *Anaeromyxobacter dehalogenans*.
584 *Biodegradation* **13**, 307-316.
- 585 Herbel M.J., Johnson T.M., Oremland R.S., Bullen T.D. (2000) Fractionation of selenium
586 isotopes during bacterial respiratory reduction of selenium oxyanions. *Geochim.*
587 *Cosmochim. Acta* **64**, 3701-3709.
- 588 Heumann K.G. (1992) Isotope dilution mass spectrometry. *Int. J. Mass Spectrom.* **118-119**,
589 575-592.
- 590 Howard H.J. (1977) Geochemistry of selenium: Formation of ferroselite and selenium
591 behavior in the vicinity of oxidizing sulfide and uranium deposits. *Geochim.*
592 *Cosmochim. Acta* **41**, 1665-1678.
- 593 Hunter W.J., Manter D.K. (2008) Bio-reduction of selenite to elemental red selenium by
594 *Tetrathibacter kashmirensis*. *Curr. Microbiol.* **57**, 83-88.
- 595 Hunter W.J., Manter D.K. (2009) Reduction of selenite to elemental red selenium by
596 *Pseudomonas* sp. strain CA5. *Curr. Microbiol.* **58**, 493-498.

- 597 Kessi J., Hanselmann K.W. (2004) Similarities between the abiotic reduction of selenite with
598 glutathione and the dissimilatory reaction mediated by *Rhodospirillum rubrum*.
599 *Appl. Environ. Microbiol.* **65**, 4734-4740.
- 600 Kipp M.A., Stueken E.E., Bekker A., Buick R. (2017) Selenium isotopes record extensive
601 marine suboxia during the Great Oxidation Event. *Proc. Natl. Acad. Sci.* **114**, 875-
602 880.
- 603 Kuroda M., Yamashita M., Miwa E., Imao K., Fujimoto N., Ono H., Nagano K., Sei K., Ike
604 M. (2011). Molecular cloning and characterization of the *srdBCA* operon, encoding
605 the respiratory selenate reductase complex, from the selenate-reducing bacterium
606 *Bacillus selenatarsenatis* SF-1. *J. Bacteriol.* **193**, 2141-2148.
- 607 Lemly A.D. (2004) Aquatic selenium pollution is a global environmental safety issue.
608 Selenium transport and bioaccumulation in aquatic ecosystems: A proposal for water
609 quality criteria based on hydrological units. *Ecotoxicol. Environ. Safe.* **42**, 150-156.
- 610 Ma, J., Kobayashi, D.Y., Yee, N. 2009. Role of menaquinone biosynthesis genes in selenate
611 reduction by *Enterobacter cloacae* SLD1a-1 and *Escherichia coli* K12. *Environ.*
612 *Microbiol.* **11**, 149-158.
- 613 Macy, J.M., Rech, S., Auling, G., Dorsch, M., Stackebrandt, E., Sly, L.I. 1993. *Thauera*
614 *selenatis* gen. nov., sp. nov., a member of the beta subclass of Proteobacteria with a
615 novel type of anaerobic respiration. *Int. J. Syst. Bacteriol.* **43**, 135-142.
- 616 Mars J.C. and Crowley J.K. (2003) Mapping mine wastes and analyzing areas affected by
617 selenium-rich water runoff in southeast Idaho using AVIRIS imagery and digital
618 elevation data. *Remote Sens. Environ.* **84**, 422-436.
- 619 Martin A.J., Simposon S., Fawcett S., Wiramanaden C.
620 I.E., Pickering I.J., Belzile N., Chen Y.W., London J., Wallschaeger D. (2011).
621 Biogeochemical mechanisms of selenium exchange between water and sediments in
622 two contrasting lentic environments. *Environ. Sci. Technol.* **45**, 2605-2612.
- 623 Mitchell, K., Mason, P.R.D., van Cappellen, P., Johnson, T.M., Gill, B.C., Owens, J.D., Diaz,
624 J., Ingall, E.D., Reichart, G.J., Lyons, T.W. 2012. Selenium as paleo-oceanographic
625 proxy: A first assessment. *Geochim. Cosmochim. Acta* **89**, 302-317.
- 626 Meseck S. and Cutter G (2012) Selenium behavior in San Francisco Bay sediments
627 *Estuaries Coast* **35**: 646-657.
- 628 Mitchell, K., Mansoor S.Z., Mason, P.R.D., Johnson, T.M., van Cappellen, P. (2016)
629 Geological evolution of the marine selenium cycle: Insights from the bulk shale
630 $\delta^{82/76}\text{Se}$ record and isotope mass balance modeling. *Earth Planet Sci. Lett.* **441**, 178-
631 187.
- 632 Muscatello J.R., Belknap A.M. and Janz D.M. (2008) Accumulation of selenium in aquatic
633 systems downstream of uranium mining operation in northern Saskatchewan, Canada.
634 *Environ. Poll.* **156**, 387-393.
- 635 Nancharaiyah Y.V., Lens P.N.L (2015) Ecology and biotechnology of selenium-respiring
636 bacteria. *Microbiol. Mol. Biol. Rev.* **79**, 61-80.
- 637 Oremland R.S., Hollibaugh J.T., Maest A.S., Presser T.S., Miller L., Culbertson C. (1989)
638 Selenate reduction to elemental selenium by anaerobic bacteria in sediments and
639 culture: Biogeochemical significance of a novel, sulfate-independent respiration.
640 *Appl. Environ. Microbiol.* **55**, 2333-2343.
- 641 Parida K.M., Gorai B., Das N.N. and Rao S.B. (1997) Studies on ferric oxide hydroxides: III.
642 Adsorption of selenite (SeO_3^{2-}) on different forms of iron oxyhydroxides. *J. Coll.*
643 *Interf. Sci.* **185**, 355-362.
- 644 Peak D. (2006) Adsorption mechanisms of selenium oxyanions at the aluminum oxide/water
645 interface. *J. Coll. Interf. Sci.* **303**, 337-345.

- 646 Peak, D. and Sparks D.L. (2002) Mechanisms of selenate adsorption on iron oxides and
647 hydroxides. *Environ. Sci. Technol.* **36**, 1460-1466.
- 648 Pearce C.I., Patrick R.A.D., Law N., Charnock J.M., Coker V.S., Fellows J.W., Oremland
649 R.S., and Lloyd J.R. (2009) Investigating different mechanisms for biogenic selenite
650 transformations: *Geobacter sulfurreducens*, *Shewanella oneidensis* and *Veillonella*
651 *atypical*. *Environ. Technol.* **30**, 1313-1326.
- 652 Pogge von Strandmann P.A.E., Stüeken E.E., Elliot T., Poulton S.W. Dehler C.M., Canfield
653 D.E., Catling D.C. (2015) Selenium isotope evidence for progressive oxidation of the
654 Neoproterozoic biosphere. *Nature Commun.* **6**.
- 655 Presser T.S. and Ohlendorf H.M. (1987) Biogeochemical cycling of selenium in San Joaquin
656 Valley, California, USA. *Environ. Managem.* **11**, 805-821.
- 657 Ridley H., Watts C.A., Richardson D.J. and Butler C.S. (2006) Resolution of distinct
658 membrane-bound enzymes from *Enterobacter cloacae* SLD1a-1 that are responsible
659 for selective reduction of nitrate and selenate oxyanions. *Appl. Environ. Microbiol.*
660 **72**, 5173 - 5180.
- 661 Sabaty M., Avazeri C., Pignol D., Vermeglio A. (2001) Characterization of the reduction of
662 selenate and tellurite by nitrate reductases. *Appl. Environ. Microbiol.* **67**, 5122-5126.
- 663 Schilling K., Johnson T.M. and Mason P.R.D. (2014) A sequential extraction technique for
664 mass-balanced stable selenium isotope analysis of soil samples. *Chem. Geol.* **381**,
665 125-130.
- 666 Schilling, K., Johnson T.M., Dhillon K.S. and Mason P.R.D. (2015) Fate of selenium in soils
667 at a seleniferous site recorded by high precision Se isotopes measurements. *Environ.*
668 *Sci. Technol.* **49**, 9690-9698.
- 669 Shrimpton H.K., Jamieson-Hanes J.H., Ptacek C.J., Blowes D.W. (2018) Real-time XANES
670 measurement of Se reduction by zerovalent iron in a flow-through cell, and
671 accompanying Se isotope measurements. *Environ. Sci. Technol.* **52**, 9304-9310.
- 672 Schröder I., Rech S., Krafft T. and Macy J.M. (1997) Purification and characterization of the
673 selenate reductase from *Thauera selenatis*. *J. Biol. Chem.* **272**, 23765-23768.
- 674 Scott K., Lu X., Cavanaugh C. and Liu J. (2004) Optimal methods for estimating kinetic
675 isotope effects from different forms of the Rayleigh distillation equation. *Geochim.*
676 *Cosmochim. Acta* **68**, 433-442.
- 677 Sikora E.R., Johnson T.M. and Bullen T.D. (2008) Microbial mass-dependent fractionation
678 of chromium isotopes. *Geochim. Cosmochim. Acta.* **72**, 3631-3641.
- 679 Stillings L.L. and Amacher M.C. (2010). Kinetics of selenium release in mine waste from the
680 Meade Peak Phosphatic Shale, Phosphoria Formation, Wooley Valley, Idaho, USA.
681 *Chem. Geol.* **269**, 113-123.
- 682 Stolz J.F. and Oremland R.S. (1999) Bacterial respiration of arsenic and selenium. *FEMS*
683 *Microbiol. Rev.* **23**, 615-627.
- 684 Stolz J.E., Basu P., Santini J.M. and Oremland R.S. (2006) Arsenic and selenium in microbial
685 metabolism. *Annu. Rev. Microbiol.* **60**, 107-130.
- 686 Stüeken E.E., Buick R., Bekker A., Catling D., Foriel J., Guy B.M., Kah L.C., Machel H.G.,
687 Montanez I.P., Poulton S.W. (2015a). The evolution of the global selenium cycle:
688 Secular trends in Se isotopes and abundances. *Geochim Cosmochim. Acta* **162**, 109-
689 125.
- 690 Stüeken E.E., Buick R., Anbar A.D. (2015b) Selenium isotopes support free O₂ in the latest
691 Archean. *Geology* **43**, 259-262.

- 692 Switzer-Blum J.S., Bindi A.B., Buzzelli J., Stolz J.F. Oremland, R.S. (1998) *Bacillus*
693 *arsenicosenenatis*, sp. Nov., and *Bacillus selenitireducens*, sp. Nov.: two
694 haloalkaliphiles from MonoLake, California that respire oxyanions of selenium and
695 arsenic. *Arch. Microbiol.* **171**, 19-30.
- 696 Theissen J. and Yee, N. (2014) The molecular basis for selenate reduction in *Citrobacter*
697 *freundii*. *Geomicrobiol. J.* **31**, 875 - 883.
- 698 Watts C.A., Ridley H., Condie K.L., Leaver J.T., Richardson D.J. and Butler C.S. (2003)
699 Se(VI) reduction by *Enterobacter cloacae* SLD1a-1 is catalysed by a molybdenum-
700 dependent membrane-bound enzyme that is distinct from the membrane-bound nitrate
701 reductase. *FEMS Microbiol. Lett.* **228**, 273-279.
- 702 Wen H.J. and Carignan J. (2011) Selenium isotope trace the source and redox processes in
703 the black shale-hosted Se-rich deposit in China. *Geochim. Cosmochim. Acta* **75**, 1411-
704 1427.
- 705 Wen H.J., Carignan J., Chu X., Fan, H.F., Cloquet C., Huang J., Zhang, Y. and Chang, H.
706 (2014) Selenium isotopes trace anoxic and ferruginous seawater conditions in the
707 Early Cambrian, *Chem. Geol.* **390**, 164-172.
- 708 Yee N. and Kobayashi, D.Y. (2008) Molecular genetics of selenate reduction by
709 *Enterobacter cloacae* SLD1a-1. *Advan. Appl. Microbiol.* **64**, 107-123.
- 710 Zhang Q., Amor K., Galer S.J.G., Thompson I., Porcelli D. (2019) Using stable isotope
711 fractionation factors to identify Cr(VI) reduction pathways: Metal-minerals-microbe
712 interaction. *Water Res.* **151**, 98-109.
- 713 Zhu J.M., Johnson T.M., Clark S.K. and Zhu X.K. (2008) High precision measurements of
714 selenium isotopic composition by hydride generation multiple collector inductively
715 coupled plasma mass spectrometry with a ⁷⁴Se-⁷⁷Se double spike. *Chin. J. Anal.*
716 *Chem.* **36**, 1385-1390.
- 717 Zhu J.M., Johnson T.M., Clark S.K., Zhu X.K., Wang X. (2014) Selenium redox cycling
718 during weathering of Se-rich shales: A selenium isotope study. *Geochim. Cosmochim.*
719 *Acta* **126**, 228-249.
- 720

721

Figure Caption

722 **Figure 1.** Phylogenetic tree showing currently described Se(VI) and Se(IV)-reducing bacteria
723 Species names are shown in italics. Red marked species represent the bacterial strains studied
724 in this work. Also indicated the taxonomic classes of bacteria.

725

726 **Figure 2.** Time series (batch experiments) of Se(VI) reduction at 30°C with 500 μM of
727 acetate (*Enterobacter cloacae SLD1a-1*) or lactate (*Desulfitobacterium chlororespirans*
728 *Co23*, *Desulfitobacterium sp. Viet-1*) as electron donor. Heat kill control with cells from
729 *Desulfitobacterium chlororespirans* Co23 incubated at 30°C with 500 μM of acetate. The
730 analytical uncertainty Se concentration is less than 1% and close to the size of the symbols.

731

732 **Figure 3.** Values of $\delta^{82/76}\text{Se}$ of Se(VI) versus remaining Se(VI) during microbial reduction in
733 closed system (batch experiments) Modelled lines (dashed) follow a predicted Rayleigh
734 fractionation process. Uncertainties (± 2 SD) are close to the size of the symbols. For the heat-
735 kill control the error bars show the root mean square error (RMS) of replicate measurements
736 as described in section 2.5.

737

738 **Figure 4.** Normalized cell-specific reduction rate (cSRR) and Se isotopic fractionation (ϵ) by
739 phylogenetically diverse bacteria **(A)** reduction of Se(VI) and **(B)** reduction of Se(IV). The
740 error bars correspond to standard deviation (± 2 SD) of ϵ 's from duplicate batch experiments
741 (x-axis), and error (%) of cSRR calculated from repeated cell-counting measurements (y-
742 axis). For some data points, the error bars are within the size of the symbol.

743

744 **Figure 5.** TEM images of *Enterobacter cloacae SLD1a-1* grown at 30°C under anoxic
745 conditions in presence of acetate as electron donor and **(A)** Se(VI) or **(B)** Se(IV). Red arrows
746 indicate the presence of intracellular (A) or extracellular (B) Se(0) as reduction product.
747 Scale bars represent 0.2 μM.

748

749 **Figure 6.** Time series (batch experiment) of Se(VI) reduction at 30°C with 500 μM of lactate
750 (*Desulfitobacterium chlororespirans* Co23, *Desulfitobacterium sp. Viet-1*, *Shewanella sp.*
751 (NR)) or acetate (*Enterobacter cloacae SLD1a-1*, *Anaeromyxobacter* FRC-W, *Geobacter*
752 *sulfurreducens* PCA,) as electron donor. The analytical uncertainty Se concentration is less
753 than 1% and close to the size of the symbols.

754 **Figure 7.** Values of $\delta^{82/76}\text{Se}$ of Se(IV) versus remaining Se(IV) during microbial reduction in
755 closed system (batch experiments). Modelled lines (dashed) show predicted Rayleigh
756 fractionation. Uncertainties (± 2 SD) are close to the size of the symbols.

Table 1. List of bacterial strains investigated in this study

Bacterial strain	Gram strain	Electron acceptor	Electron donor
<i>Enterobacter cloacae</i> SLD1a-1	-	Se(VI)/Se(IV)	Acetate
<i>Desulfitobacterium chlororespirans</i> Co23	+	Se(VI)/Se(IV)	Lactate
<i>Desulfitobacterium sp.</i> Viet-1	+	Se(VI)/Se(IV)	Lactate
<i>Geobacter sulfurreducens</i> PCA	-	Se(IV)	Acetate
<i>Anaeromyxobacter dehalogenans</i> FRC-W	-	Se(IV)	Acetate
<i>Shewanella sp.</i> (NR)	-	Se(IV)	Lactate

Table 2. Reduction rate [$t_{50\%}$ in days] and cell-specific reduction rate (cSRR) of investigated bacterial strains

Bacterial strain	Electron acceptor	Initial Se (μM)	Time for 50% reduction ($t_{50\%}$) (d)	Normalized cSRR (10^{-17} mol cell $^{-1}$ d $^{-1}$)
<i>Enterobacter cloacae</i> SLD1a-1	Se(VI)	30	1.13	0.24
	Se(IV)	9	1.03	5.68
<i>Desulfitobacterium chlororespirans</i> Co23	Se(VI)	42	41.25	0.11
		9	2.31	0.29
			1.27	0.45
	Se(IV)	9	0.42	0.51
			0.71	0.31
<i>Desulfitobacterium sp.</i> Viet-1	Se(VI)	47	1.10	0.34
			0.79	1.22
		13	3.80	0.98
			3.85	1.30
	Se(IV)	9	3.10	0.65
			2.49	0.85
<i>Geobacter sulfurreducens</i> PCA	Se(IV)	13	3.10	0.28
		8	0.49	0.92
			0.66	1.14
		15	0.63	0.81
			0.55	1.32
<i>Anaeromyxobacter dehalogenans</i> FRC-W	Se(IV)	13	0.51	0.78
<i>Shewanella sp.</i> (NR)	Se(IV)	19	2.37	0.53
		13	1.60	2.17

Table 3. Magnitude of isotopic fractionation ϵ of Se(VI) and Se(IV) reduction by various bacterial strains

Bacterial strain	Electron acceptor	Initial Se concentration (μM)	Electron donor concentration (μM)	ϵ (‰) $^{82/76}\text{Se}$ $\pm 2\text{s.e.}$	Number of experiments
<i>Enterobacter cloacae</i> SLD1a-1	Se(VI)	30	500	-11.5 \pm 0.5	2
	Se(IV)	9	500	-7.6 \pm 0.3	1
<i>Desulfitobacterium chlororespirans</i> Co23	Se(VI)	42	500	-11.8 \pm 0.6	1
		9	500	-11.3 \pm 0.2	2
	Se(IV)	9	500	-7.8 \pm 0.8	2
<i>Desulfitobacterium sp.</i> Viet-1	Se(VI)	47	500	-9.3 \pm 0.5	2
		13	500	-9.2 \pm 0.2	2
	Se(IV)	9	500	-7.3 \pm 0.2	2
<i>Geobacter sulfurreducens</i> PCA	Se(IV)	13	500	-6.3 \pm 0.6	2
		8	2000	-7.0 \pm 0.4	3
		15	10000	-7.3 \pm 0.5	3
<i>Anaeromyxobacter dehalogenans</i> FRC-W	Se(IV)	13	500	-6.3 \pm 0.5	1
<i>Shewanella sp.</i> (NR)	Se(IV)	19	500	-6.9 \pm 0.2	1
		13	500	-6.2 \pm 0.4	1

Figure 1

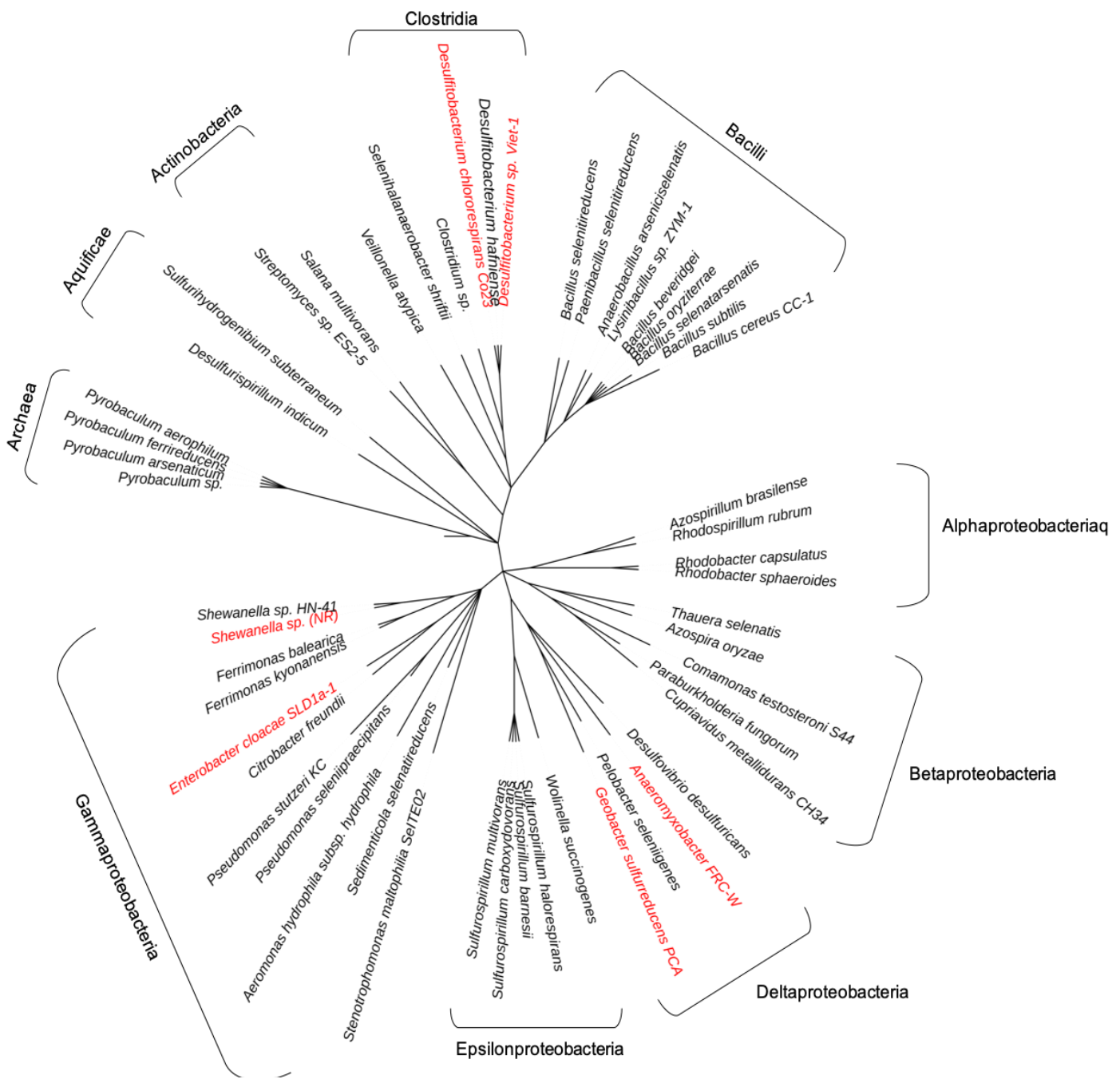


Figure 2

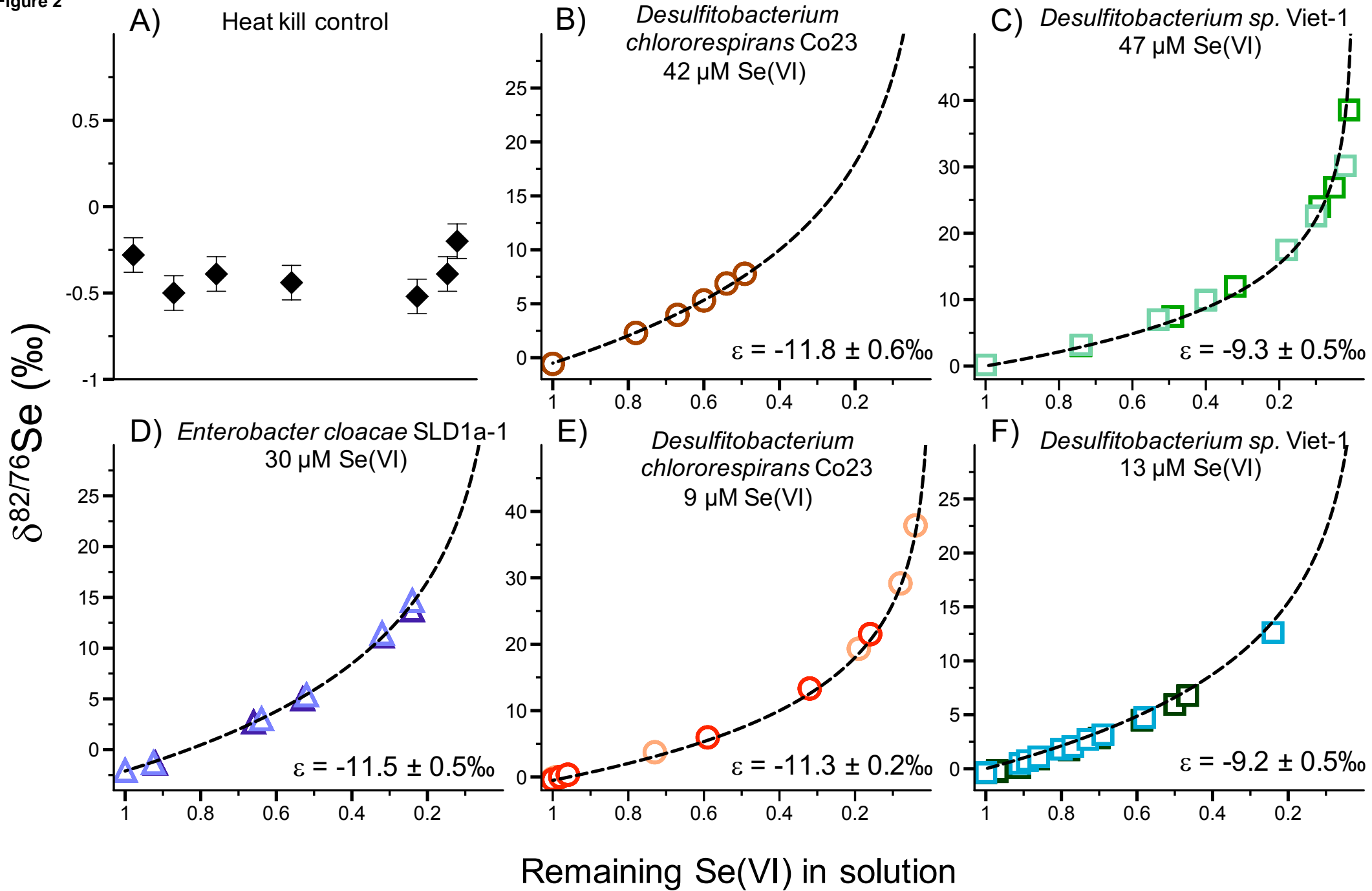


Figure 3

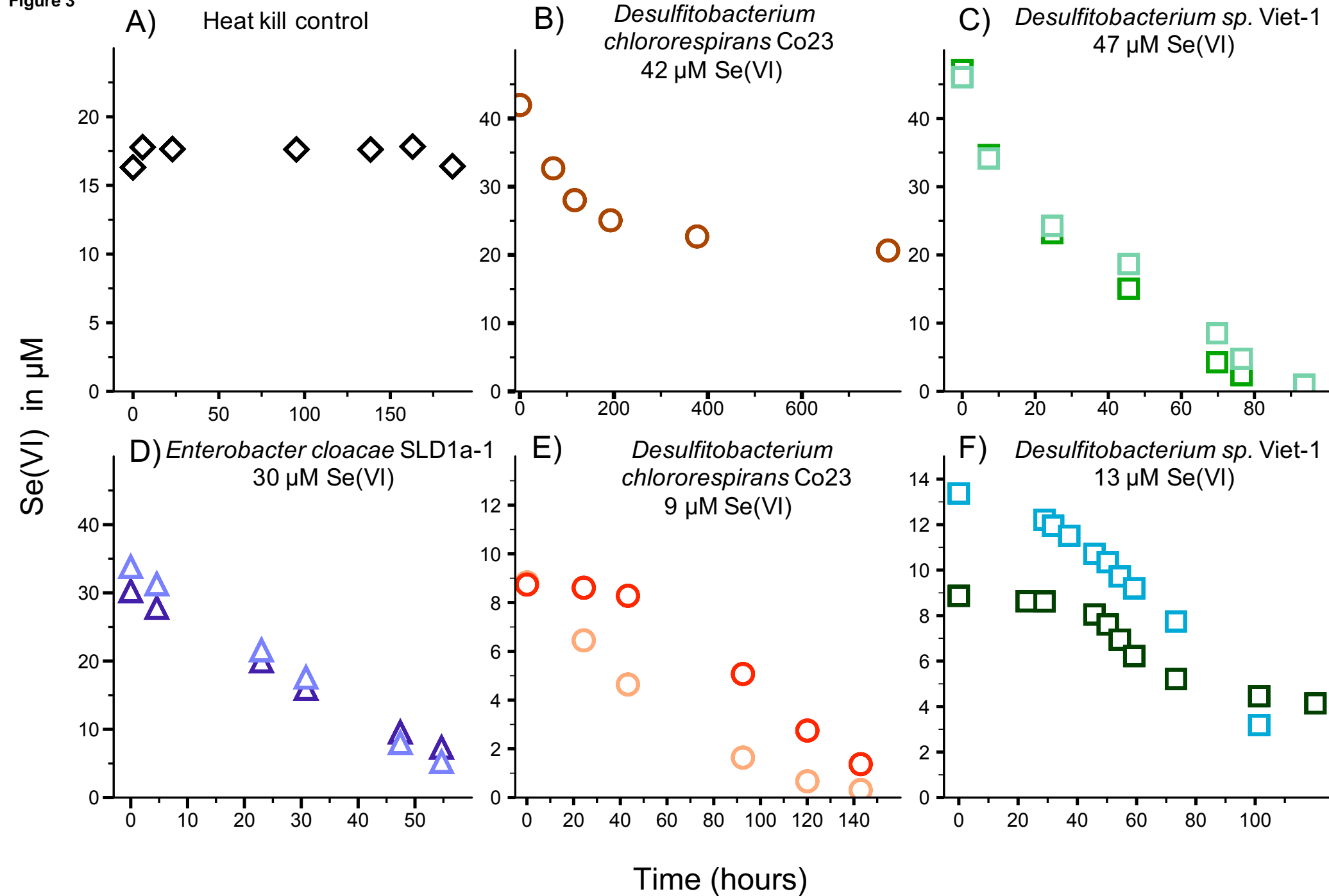


Figure 4

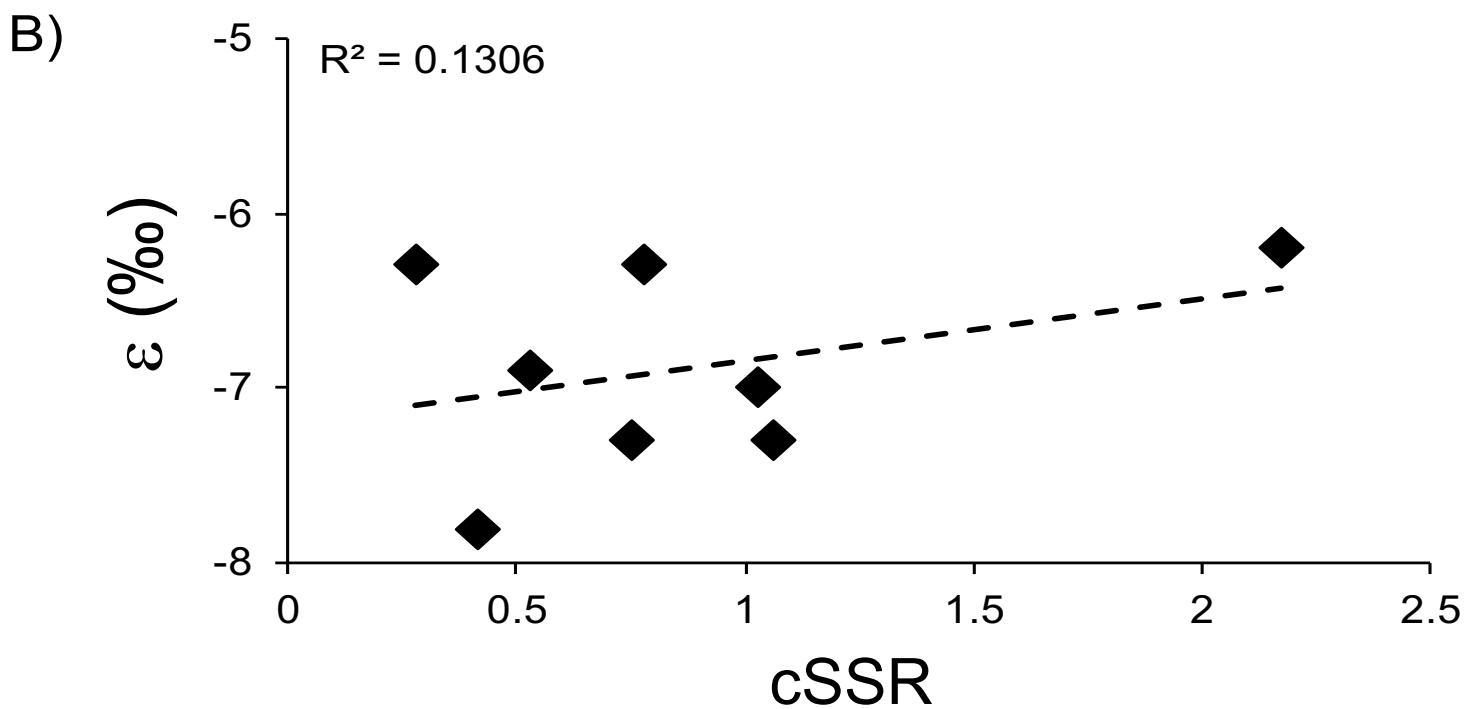
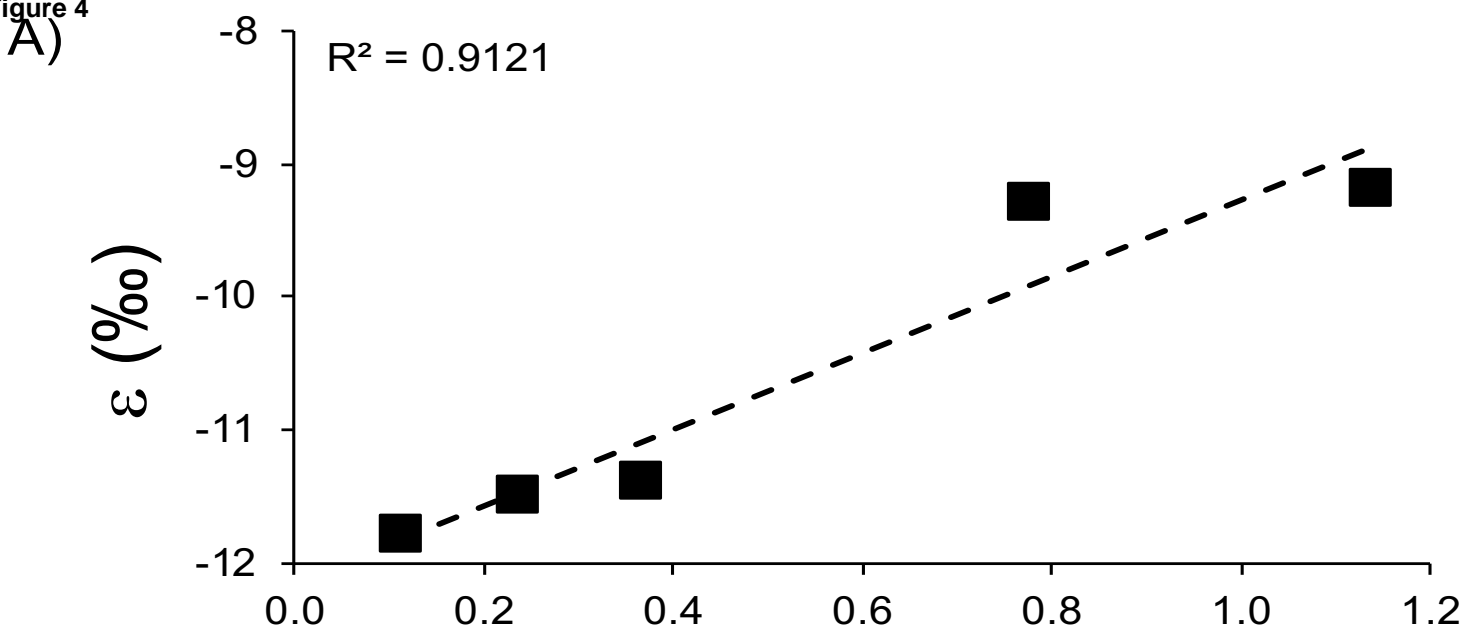


Figure 5

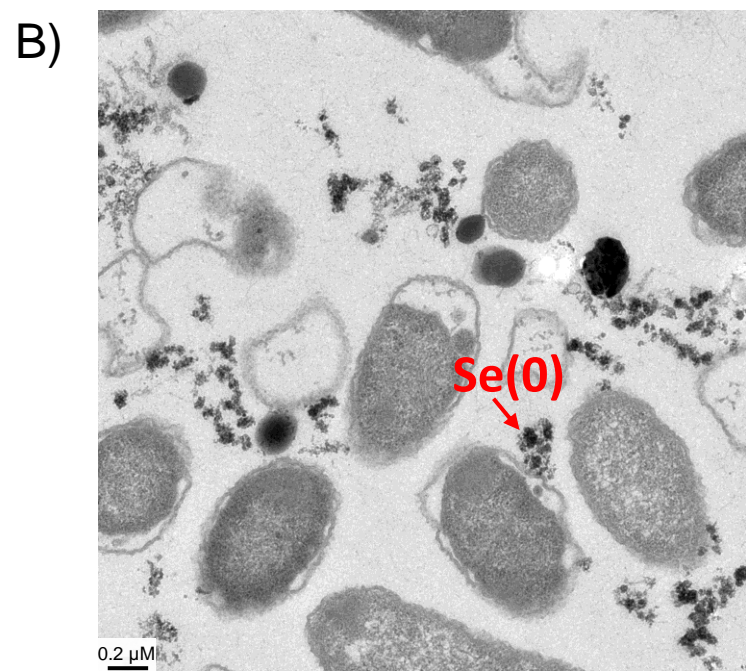
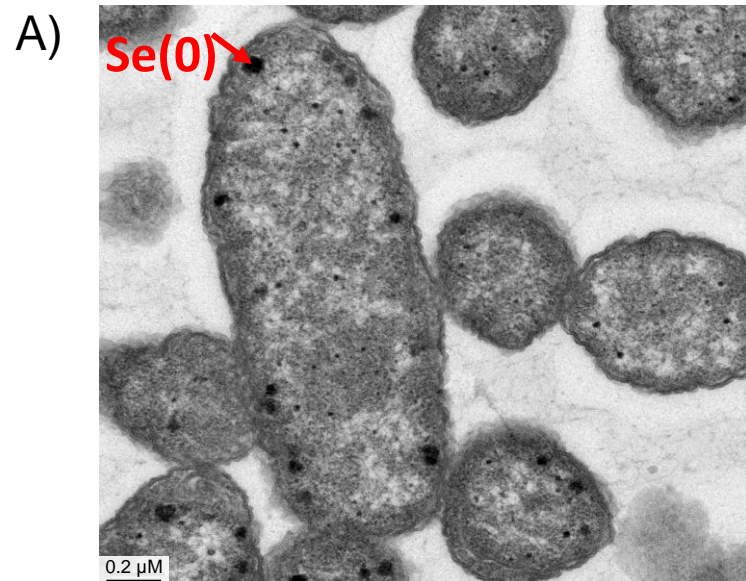


Figure 6

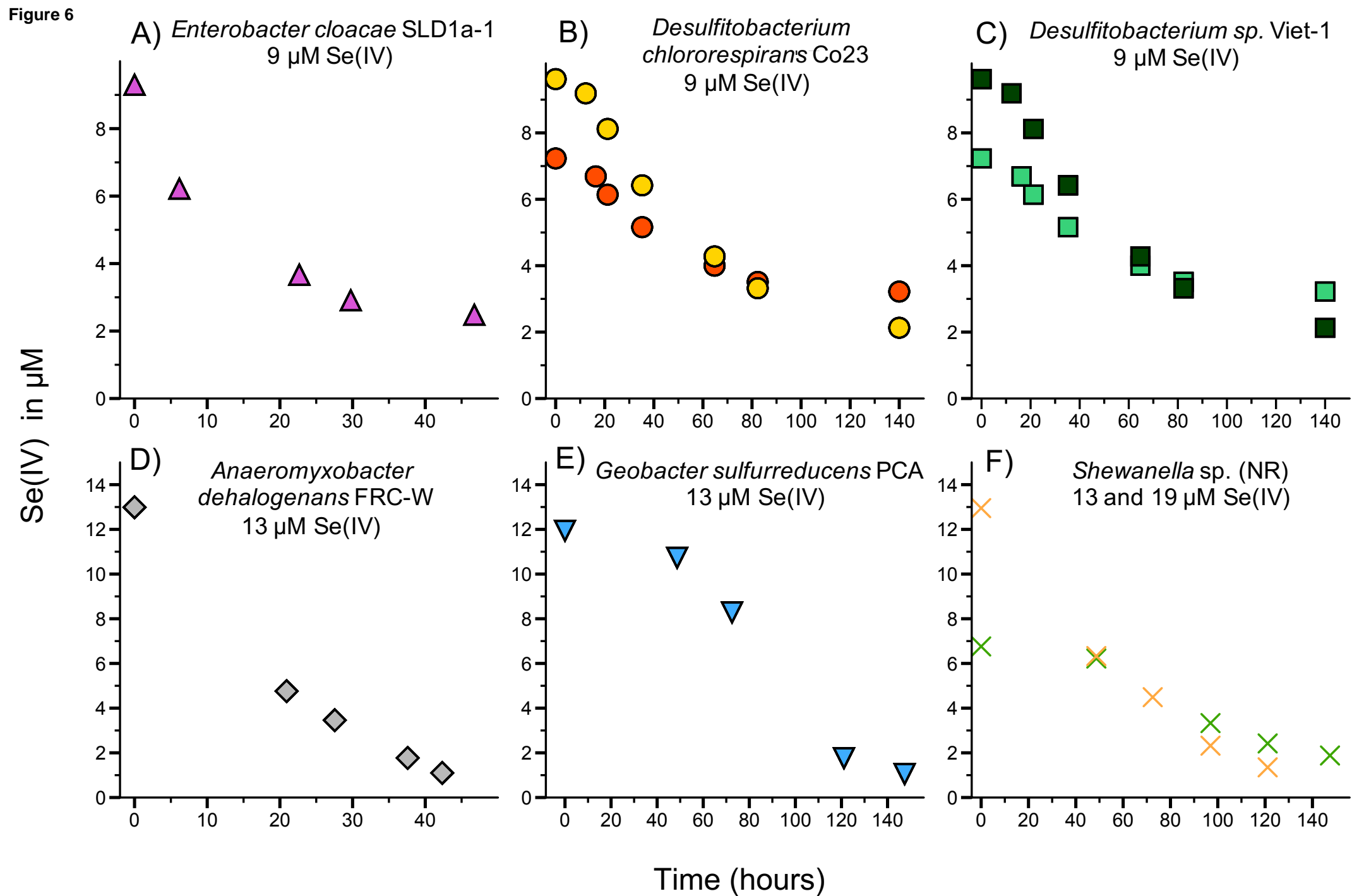
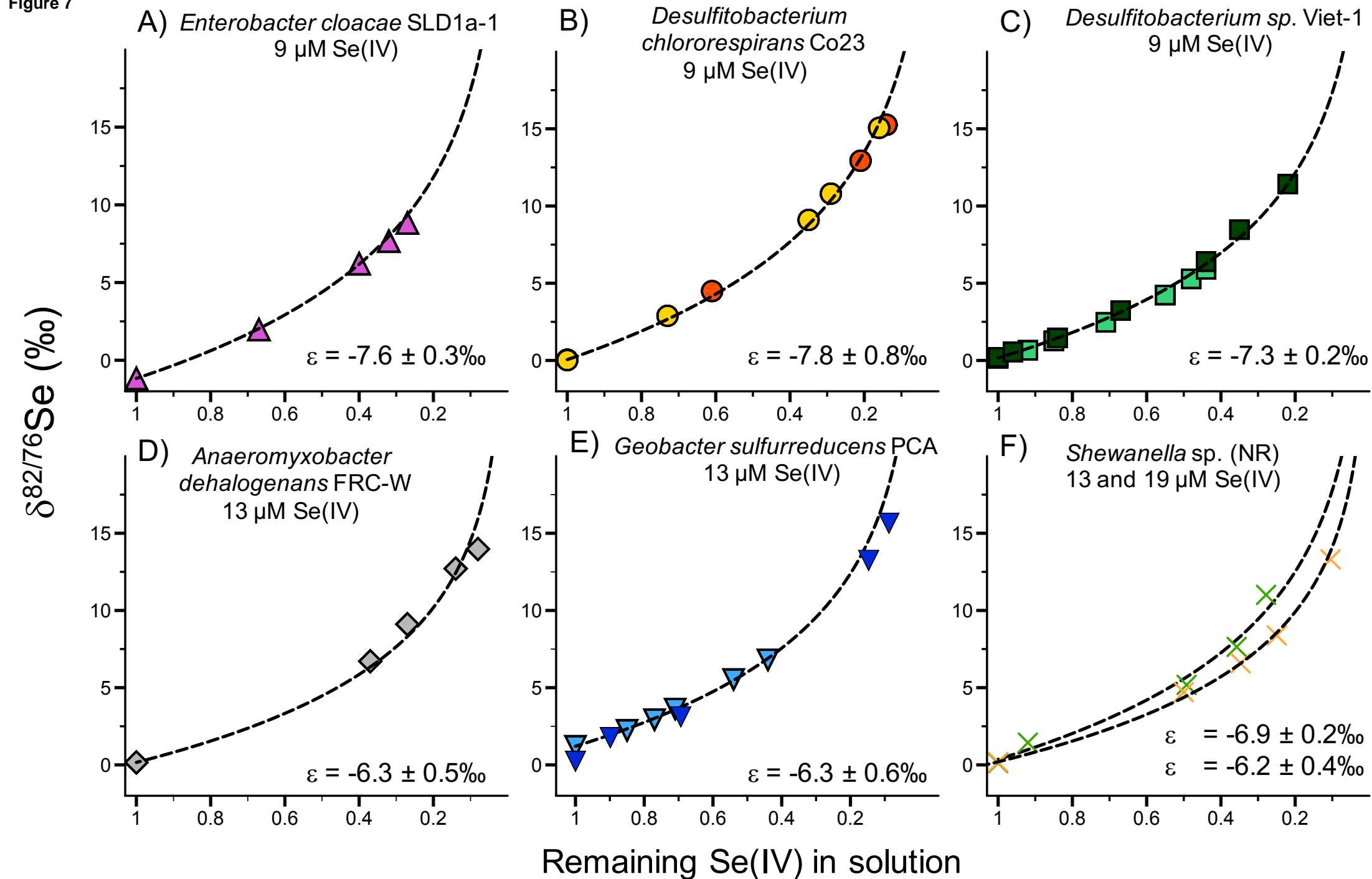


Figure 7



Electronic Annex

[Click here to download Electronic Annex: Electronic Annex_GCA.docx](#)

Appendix

[Click here to download Appendix: APPENDIX_GCA.docx](#)